SILICON PROCESSING
FOR
THE VLSI ERA

VOLUME 1:
PROCESS TECHNOLOGY
Second Edition

STANLEY WOLF Ph.D.
RICHARD N. TAUBER Ph.D.

LATTICE PRESS
Sunset Beach, California

DISCLAIMER

This publication is based on sources and information believed to be reliable, but the authors and Lattice Press disclaim any warranty or liability based on or relating to the contents of this publication.

Published by:

LATTICE PRESS
Post Office Box 340
Sunset Beach, California 90742, U.S.A.

Cover design by Roy Montibon, New Archetype Publishing, Los Angeles, CA.

Library of Congress Cataloging in Publication Data
Wolf, Stanley and Tauber, Richard N.

Silicon Processing for the VLSI Era
Volume 1: Process Technology

Includes Index
1. Integrated circuits-Very large scale integration. 2. Silicon. I. Title

ISBN 0-9616721-6-1

9 8 7 6 5 4 3 2

PRINTED IN THE UNITED STATES OF AMERICA

depth at which each ion stops is determined. The predicted profile is generated by plotting histograms of the number of ions stopped within each depth interval. Monte Carlo simulations can be performed for either amorphous or crystalline targets. In the amorphous material simulation, the position of the target atoms follows a Poisson distribution, while in crystalline target simulation the atom positions are specified to correspond to the positions that they would assume on a lattice.

A widely used, PC-based Monte Carlo range and damage simulation program is named TRIM (for Transport *of Ions in Matter*).[23] It assumes that the target material is amorphous (i.e., no channeling effects occur), and consequently provides a very useful first-approximation to the atom range and damage distributions in multi-element and multi-layer materials.[24] A more advanced Monte Carlo code has been developed for Si-like crystalline targets (UT-MARLOWE). It runs on Unix-based workstations and provides highly accurate atom range and damage distributions (including the effects of damage accumulation on channeled profiles).[84,85]

10.3 ION IMPLANTATION DAMAGE ACCUMULATION AND ANNEALING IN SILICON

As discussed earlier, ion implantation has many advantages for ULSI processing, the most important being the ability to control (to a high degree of precision) the number and depth of impurity atoms introduced into a substrate. The price for such benefits is high, however, as implantation cannot be achieved without damage to the substrate material. That is, high-energy ions collide with substrate atoms and displace them from their lattice sites in large numbers. Furthermore, only a small percentage of the as-implanted atoms end up on electrically active lattice sites. In order to successfully fabricate devices, the damaged substrate regions must be

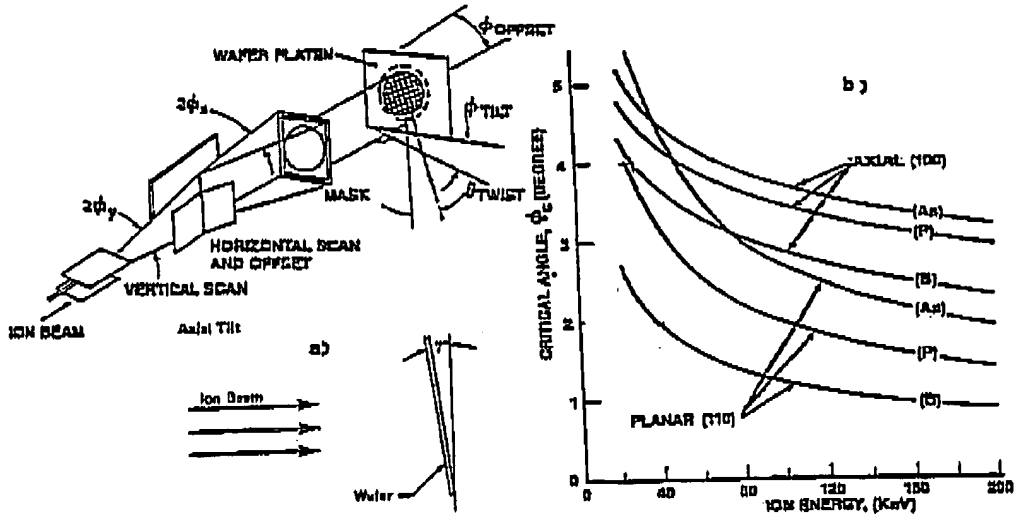

Fig. 10-13 (a) Channeling avoidance by using axial tilt and azimuthal twist. (b) Calculated critical angles vs. ion energy for channeling along the axial Si <100> direction and planar <110> direction for B^+, P^+, and As^+ ions.[13] Reprinted with permission of Solid State Technology, published by PennWell.

must be restored to their pre-implanted structure, and the implanted species must be electrically activated. Described in this section are: a) the aspects of implantation damage; b) the mechanisms of damage annealing; and c) the electrical activation of implanted dopants. Figure 10-14 illustrates the subjects that will be covered. At the conclusion of the section it will be noted that as devices are designed with very shallow junctions (e.g., ≤250 nm deep), the remaining residual implantation damage (even after the annealing process) represents a mechanism that degrades device operation. An example is the excess reverse-bias leakage current observed when such shallow junctions are fabricated.

10.3.1 Implantation Damage in Silicon

When energetic ions strike a silicon substrate they lose their energy in a series of nuclear and electronic collisions, and thus rapidly come to rest some hundreds of atom layers below the surface. Only the nuclear collisions result in *displaced silicon atoms* (also referred to as *damage* or *disorder*). An individual nuclear collision can result in different types of displacement events, depending upon the magnitude of the energy transferred.

If the energy transferred to a silicon atom (ΔE_n) is less than the energy required to displace it from its lattice site, E_{dl}, no displacement event results. If $2E_{dl} \geq \Delta E_n \geq E_{dl}$, a single displacement and simple isolated point defects are created. If $\Delta E_n \geq 2E_{dl}$, point defects and *secondary displacements* (i.e., recoiled lattice atoms with enough energy to generate additional lattice disorder) are produced. Finally, if $\Delta E_n >> 2E_{dl}$, multiple secondary displacements and defect clusters are created. (Note, E_{dl} [Si] ~15 eV.)

Because of their extremely small size, the exact nature of isolated defects and defect complexes from ion implantation are hard to characterize. However, each displacement of a lattice atom (whether by a primary beam ion or an energetic recoil lattice atom), produces a *Frenkel defect* (see Chap. 2). In addition, it is widely agreed that the defects include: a) vacancies [V]; b) di-vacancies [V^2] (i.e., two vacancies bound together); c) higher order vacancies and (vacancy-impurity complexes); and d) interstitials [I]. The ions create zones of gross disorder populated by such defects in regions where they deposit their kinetic energy (Fig. 10-15). These zones are vacancy-rich at the center, and are surrounded by [I], since each displaced Si atom moves into the lattice with velocity components perpendicular to the ion track.

The lattice in these disordered regions exhibits several different damage configurations:

1. *Isolated point defects* or *point defect clusters in essentially crystalline silicon* (i.e., the type of damage that results from implanting light ions, or when $\Delta E_n \cong 2E_{dl}$).
2. *Local zones of completely amorphous material* in an otherwise crystalline layer (i.e., an *amorphous region* is defined as a region in which the displaced atoms per unit volume approach the atomic density of the semiconductor). Local zones of amorphous damage are associated with low-dose implants of heavy ions (i.e., $\Delta E_n >> E_{dl}$).
3. *Continuous amorphous layers* which form as the damage from the ions accumulates. That is, as the dose of ions (typically heavy ions) increases, the locally amorphous regions eventually overlap, and a continuous amorphous layer is formed.

In our discussion Type-1 and Type-2 damage will be grouped into the category of *primary crystalline-defect damage*. Type-3 damage will be referred to as *amorphous layer damage*. The basis for this grouping (as shall be seen in the sections that discuss damage annealing), is that the annealing strategy for Type-1 and Type-2 damage are the same, but a different annealing procedure is employed for Type-3 damage.

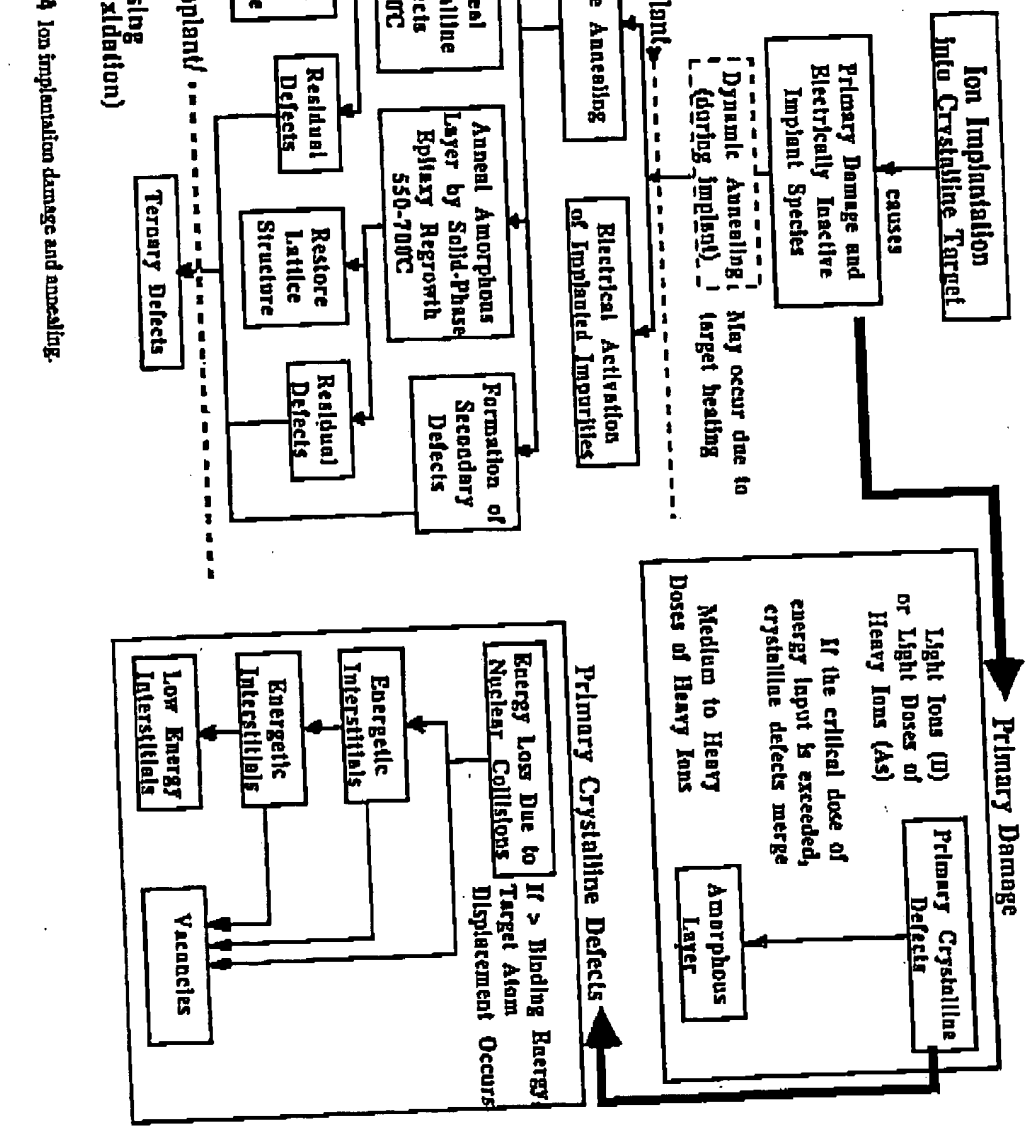

Fig. 10-14 Ion implantation damage and annealing.

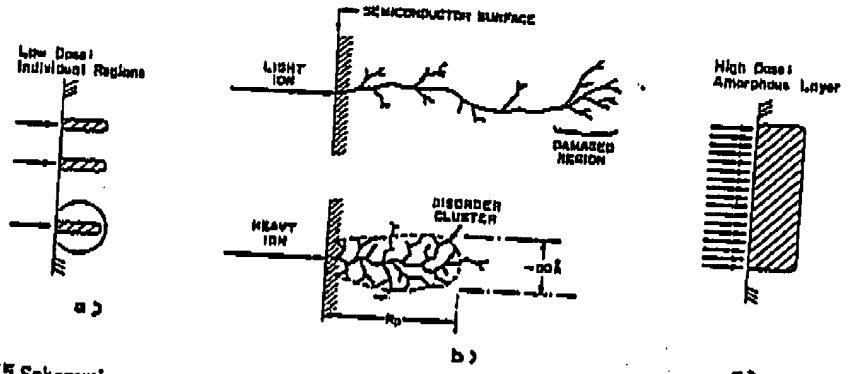

Fig. 10-15 Schematic representation of the disorder produced by ion implantation. (a) Low dose light ions - individual regions with degree of disorder increasing as ions penetrate deeper into substrate. (b) Low dose heavy ions - individual regions of more uniform disorder along entire ion trajectory. (c) Heavy doses - formation of an amorphous layer.

Regardless of the form of the damage configuration, the number of displaced atoms after implant is almost always larger than the number of implanted atoms. These displaced atoms reduce the mobility in the damaged regions and produce defect levels in the band gap of the material (i.e., deep-level traps, for both electrons and holes) which have a strong tendency to capture free carriers from the conduction and valence bands. Due to the relatively large number of displaced atoms (and the fact that few as-implanted impurities occupy substitutional sites), non-annealed implanted regions typically exhibit high resistivity.

10.3.2 Primary Crystalline Defect Damage

Primary crystalline defect damage is observed after implanting a Si crystal (28 atomic mass units [28 amu]) with relatively light ions (e.g., B [11 amu]), or with light doses of heavier ions (e.g., P [31 amu], As [75 amu], and Ar [40 amu]). As noted in the previous section, the damage configurations from light ions are in fact quite different than those from heavy ion implantation. The reason for the difference is discussed below.

As shown in Fig. 10-5, at the initial impact energies most of the energy loss for *light ions* (in this example, boron) is due to electronic collisions (which do not produce displacement damage). However, as B ions penetrate deeper into the lattice, they lose energy. Eventually, the cross-over energy is reached, below which nuclear stopping predominates (~10 keV for B). As shown in Fig. 10-15, *most lattice damage occurs in the part of the light ion trajectory beyond that point.*

An estimate of the damage can be calculated by considering the case of an 80-keV boron ion. Its projected range is ~250 nm (Fig. 10-7), and its initial *nuclear energy loss is* ~35 eV/nm (Fig. 10-5). The boron ion will thus lose ~8.75 eV from nuclear collisions for each lattice plane that it passes (as the lattice spacing in Si is ~0.25 nm). Since 8.75 eV is less than E_{di} [Si], the B atom (upon initially entering the Si), does not transfer enough energy per nuclear collision to displace silicon atoms from their lattice sites. When the ion energy has decreased, however, to 40 keV (at a depth of ~130 nm in the lattice), the energy loss due to nuclear collisions rises to ~15 eV per

lattice plane (i.e., 60 eV/nm), which is sufficient to displace Si lattice atoms. (Note that although electronic stopping is still predominant, nuclear stopping between 10–40 keV can still displace Si atoms.) Assuming that one Si atom is displaced per lattice plane for the remainder of the ion trajectory, 480 lattice atoms are displaced (i.e., 120 nm/0.25 nm) by the time the boron atom comes to complete rest. If each displaced atom is moved roughly 2.5 nm by such collisions, the damage volume is found from $V_{dam} \cong \pi\ (2.5\text{nm})^2(120\ \text{nm}) \cong 2.4\times10^{-18}\ \text{cm}^3$. The damage density is $480/V_{dam} \cong 2\times10^{20}\ \text{cm}^{-3}$, which amounts to only ~0.2% of the atoms. This calculation implies that very large doses of light ions are required to produce an amorphous layer, and for the most part each ion produces a trail of well-separated primary recoiled Si atoms in the wake of the implanted ion. Furthermore, displaced atoms will be separated by short distances from the vacancies they leave, because the energies of their recoils are low. This suggests that only a relatively small input of energy to the lattice could cause such separated pairs to rejoin. In fact, as will be explained in the following section on annealing, a large fraction of the disorder produced during boron implantations is *dynamically annealed during the implantation*, and therefore at room temperatures even high-dose boron implantations may not produce an amorphous layer. The damage from boron implantations is thus characterized by *primary crystalline defects*. Damage density is distributed versus depth as shown in Fig. 10-16a, which shows a sharp buried peak concentration and qualitatively fits the description of the damage-creation process.

When *heavy ions* are implanted, the energy loss is predominantly due to nuclear collisions over the entire range of energies experienced by the decelerating heavy ions (Figs. 10-5 and 10-15). Thus, substantial damage is expected. Examine the case of 80-keV arsenic atoms, which will have a projected range of ~50 nm. The average energy loss due to nuclear collisions will be ~1200 eV/nm over the entire range. As a result, the As atoms lose ~300 eV for each Si atomic plane that they pass. Most of this energy is transferred to a single lattice atom. The recipient Si atom, however, will subsequently produce ~20 displaced lattice atoms. The total number of displaced atoms is thus 4000. Again, assuming an average distance moved for each displaced atom of ~2.5 nm, the damage volume is $V_{dam} \cong \pi\ (2.5\ \text{nm})^2(50\ \text{nm}) = 0.8\times10^{-18}\ \text{cm}^3$. The damage density is then $4000/V_{dam} \cong 5\times10^{21}\ \text{cm}^{-3}$, or ~10% of the number of atoms in the lattice within the damage volume. Since a single ion is capable of producing such heavy damage, it is reasonable to expect that some local regions of a silicon substrate (which when subjected to even light doses of heavy-ion bombardment) will suffer enough damage to become amorphous. Some damage density distributions due to heavy-ion (e.g., As) implants are shown in Fig. 10-16b. They exhibit a *broad* buried peak that is a replica of recoiled range distribution.

10.3.3 Amorphous Layer Damage

Simple qualitative concepts illustrate how continued bombardment by heavy ions will lead to the formation of continuous amorphous layers. That is, heavy-ion damage accumulates with ion dose through an increase in the density of localized amorphous regions. Eventually these regions overlap, and a continuous amorphous layer is the result. The evolution of a continuous amorphous layer from the accumulation and overlap of damage formed by individual atoms has been observed (Fig. 10-17) using Rutherford backscattering spectroscopy in a channeling mode. In Fig. 10-17a it can be seen that damage produced by 1.7 MeV Ar^+ ions in Si builds up to an initial damage distribution with a peak at a depth of ~1.3 μm. At that depth, individual amorphous zones are likely to be created by each ion (Fig. 10-17b). Closer to the surface the damage consists predominantly of isolated defect clusters (akin to the damage caused by light

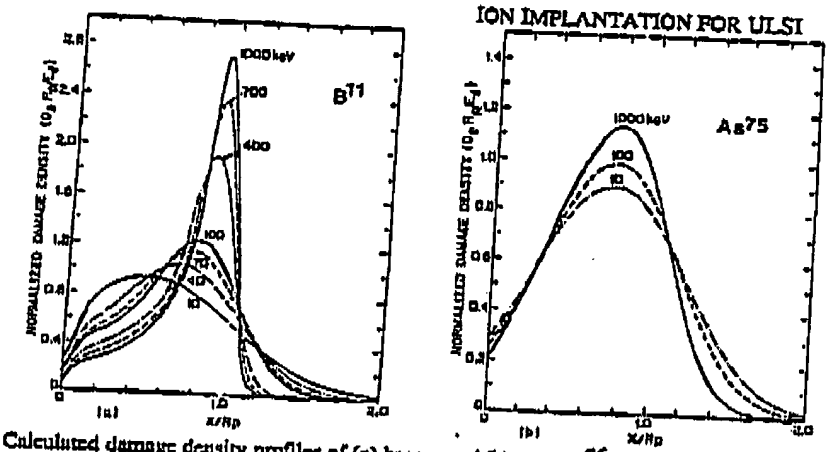

Fig. 10-16 Calculated damage density profiles of (a) boron, and (b) arsenic.[25] Reprinted with permission of Plenum Publishing Company.

ions.) As the dose is increased, both types of damage increase, and finally a 1.5 μm-thick, (almost continuous, as in the example of Fig. 10-17a) amorphous layer extends to the surface. This also illustrates another aspect of the formation of amorphous layers. That is, amorphization begins at the depth of the maximum nuclear collision energy deposition, at slightly less than the projected range, and spreads towards the surface (as well as towards deeper positions in the target). In addition, the interface with the single-crystal region below is not a well-defined plane, due to the statistical nature of the penetration. Beyond the interface, primary crystalline damage as well as a considerable concentration of Si interstitials (which had diffused out of the damage clusters during implantation) is expected.

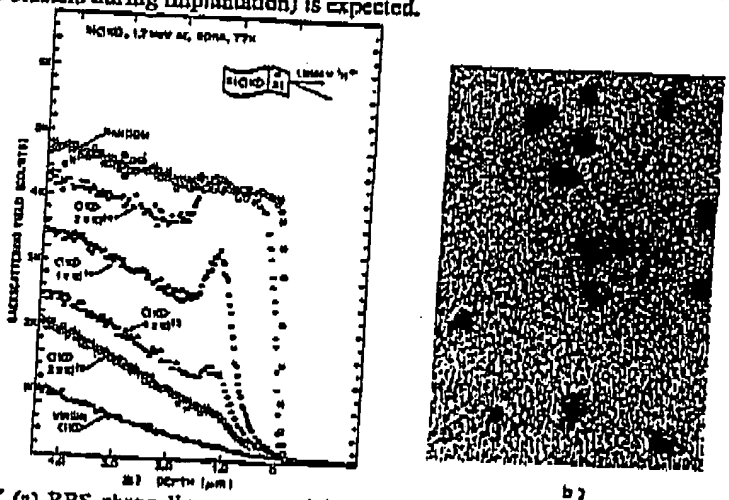

Fig. 10-17 (a) RBS channeling spectra of damage accumulation in Si at liquid nitrogen temperature following bombardment with 1.7 MeV Ar^+ ions.[26] By permission of the Harvard University Archives. (b) Bright-field electron micrographs of amorphous regions in Si produced by bombarding to doses of 3×10^{11} cm^{-2} with 10 keV bismuth ions.[27] Courtesy of the Institute of Physics Conference Series.

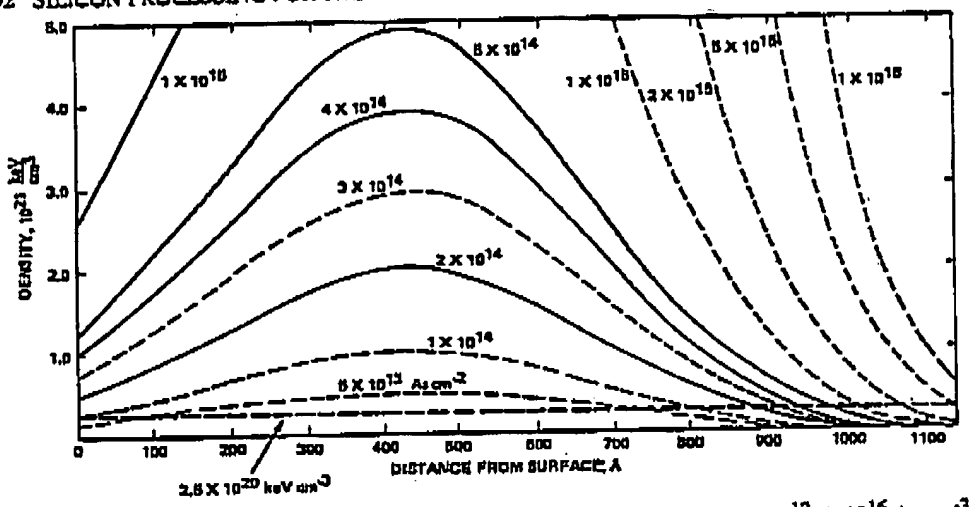

Fig. 10-18 Damage density distribution for 100-keV As implantations for doses of $5x10^{13}$–$1x10^{16}$ As cm^{-3} calculated from Brices[25] curves.[28] Reprinted by permission of American Physical Society.

The minimum (or *threshold*) dose required to convert a crystalline material to an amorphous layer can be arrived at from a number of different viewpoints. First, it is certain that when the number of stably displaced Si atoms reaches the number of Si atoms/unit volume (e.g., $5x10^{22}$ cm^{-3}), the material has become "amorphous." When the damage density reaches this value, an amorphous condition is reached. Another view holds that there is a critical energy density that must be placed into the crystal to make it amorphous.[29] This critical energy E_c is given by:

$$E_c \cong f\,(10^{21}\ \text{keV})/\text{cm}^3 \qquad (10.12)$$

and the pre-factor f is 0.1–0.5 for Si. Based on this model, Brice published tables that predict the extent of the amorphous layer formation for different doses (and constant implant energy). Prussin *et al.*[28] plotted the data from these tables for As implanted into Si (Fig. 10-18). A simple estimate can also be obtained by assuming that if enough energy is applied to the crystal to cause melting (for Si, 10^{21} keV/cm^3); this would also produce an amorphous layer. For 100-keV As ions, the dose D_{crit} calculated from this approach (where E_o is the beam energy in keV, and R_p in cm), is:

$$D_{crit} = [(10^{21}\ \text{keV/cm}^3)\,R_p]/E_o = 6x10^{13}\ \text{ions/cm}^2 \qquad (10.13)$$

From the discussion on minimum implant dose for creating an amorphous layer, three more important aspects of amorphous layer structure can be inferred:

1. From Brice's model (Fig. 10-18), it can be seen that some implant doses will cause an amorphous layer to form below the surface of the Si, but that near the surface not enough energy has been transferred to the lattice to cause the material to become amorphous (e.g., in the case of As at 100 keV, for doses less than $1x10^{14}$ cm^{-2}, the energy density at the surface drops below the threshold required to create an amorphous layer). Thus the amorphous region does not extend all the way to the surface, but is a *buried amorphous layer*. Such buried amorphous layers have been found to exhibit profoundly different annealing characteristics than those that extend all the way to the surface.

2. In the crystalline layer just below the amorphous layer, the silicon was the recipient of impurity atoms, albeit in lower quantities than necessary to cause an amorphous region. Yet, heavy primary-crystalline-defect damage from the implanted ions exists in this zone, as well as implanted impurity atoms that must be electrically activated in order to achieve the full electrical activation of the dose. These cannot be ignored when considering an annealing strategy for amorphous layers.

3. Prussin *et al.*,[28] have shown that the critical energy, E_c, required to create an amorphous layer depends on the implanted species, and is 2.5×10^{20} keV/cm^3, 1.0×10^{21} keV/cm^3, and 5.0×10^{21} keV/ cm^3, for As, P, and B, respectively.

The temperature of the substrate during implantation also impacts amorphous layer formation. Figure 10-19 shows a plot of the critical dose versus reciprocal temperature for various ions.[28] It can be seen that for light ions such as B^{11}, a 50°C rise above room temperature prevents the formation of an amorphous layer at any dose. This is due to the fact that B generates only a few stably displaced atoms during implantation, and a small increase in T above room temperature allows such closely spaced vacancy-interstitial pairs (Frenkel defects) to recombine.

10.3.4 Electrical Activation and Implantation Damage Annealing

In this section the methods that can be used in attempts to restore the silicon to its pre-implanted structure, and to electrically activate the implanted impurity atoms are considered. The subjects will be covered in the following order: a) electrical activation of implanted impurities; b) annealing primary crystalline defect damage; c) annealing of amorphous layers; d) dynamic annealing effects; and e) diffusion of implanted impurities.

10.3.4.1 Electrical Activation of Implanted Impurities: Since most as-implanted impurities do not occupy substitutional sites, a subsequent thermal step is employed to bring about electrical activation. The degree to which the thermal procedure is effective in electrically activating impurities is commonly determined by Hall effect measurements, but can also be checked more simply by measuring the sheet resistance, R_S.[30] To a first approximation, R_S is inversely proportional to the mobility μ and the implanted dose ϕ (cm^{-2}):

$$R_S \propto 1/(q\,\mu\,\phi) \qquad (10.14)$$

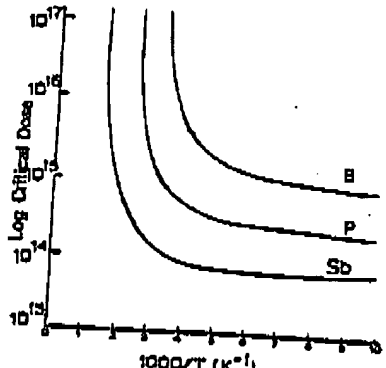

Fig. 10-19 Theoretical relationship between amorphous threshold and temperature for B^+, P^+, and Sb^+ into Si.[29] Reprinted with permission of Gordon and Breach Publishing Company.

where q is the electronic charge. Although μ depends strongly on the concentration of doping atoms and implantation damage, values of R_S have been tabulated utilizing known mobility data.[31] For a known dose, full electrical activity is reached when the predicted R_S is reached.

Electrical activation of implanted impurities in amorphous layers proceeds differently than in layers with primary crystalline damage. As will be discussed, electrical activation in amorphous layers occurs as the impurities in the layer are incorporated onto lattice sites during recrystallization. Electrical activation in crystalline damaged regions exhibits more complex behavior.

For example, Fig. 10-20 shows the *isochronal* electrical activation behavior of implanted boron (i.e., anneals performed at varying temperatures, but for identical times). In this curve, the measured surface carrier concentration (normalized for different junction depths to the dose, in cm^{-2}) is used to indicate the degree of activation. That is, when $p_{Hall}/\phi = 1$, full activation is reached. Note that other impurities exhibit similar behavior to that shown in Fig. 10-20, provided the implantation does not cause a continuous amorphous layer to be formed.

The temperature range up to 500°C (Region 1 of Fig. 10-20) shows a monotonic increase in electrical activity. This is due to the removal of trapping defects and the concomitant large increase in free carrier concentration as the traps release the carriers to the valence or conduction bands. In Region 2 (500–600°C), substitutional B concentration actually decreases. This is postulated to occur as a result of the formation of dislocations at these temperatures. Some boron atoms that were already on substitutional sites are believed to precipitate on or near these dislocations. In Region 3 (>600°C), the electrical activity increases until full activation is achieved at temperatures ~800–1000°C. The higher the dose, the more disorder, and the higher the final temperature required for full activation. At such elevated temperatures, Si self-vacancies are generated. They migrate to the B precipitates, allowing boron to dissociate and fill the vacancy (i.e., a substitutional site).

Activation of implanted impurities by rapid thermal processing (RTP, see Chap. 9) has also been studied. The time-temperature cycle to reach minimum sheet resistance for As, P, and B is ~5–10 sec at 1000–1200°C, the exact condition being dependent on implanted species, energy, and dose.[33,34]

10.3.4.2 Annealing of Primary Crystalline Damage: Isolated point defects and point defect clusters (that predominantly occur during light ion implantation), and locally amorphous zones (that are typically observed from light doses of heavy ions), are both regions of primary crystalline damage that exhibit comparable annealing behavior. At low temperatures (up to ~500°C), vacancies and self-interstitials that are in close proximity undergo recombination, thereby removing trapping defects. At higher temperatures (500–600°C), as described above, dislocations start to form, and these can capture impurity atoms. Temperatures of 900–1000°C are required to dissolve these dislocations. Note that the activation energy of impurity diffusion in Si is always smaller than that of Si self-diffusion (see Chap. 9). Therefore, the ratio of defect annihilation to the rate of impurity diffusion becomes greater as the temperature is raised. This implies that *the higher the anneal temperature the better*, with the upper limit being constrained by the maximum allowable junction depth dictated by the device design.[30]

It is also important that the steps used to anneal implantation damage be conducted in a neutral ambient, such as Ar or N_2. That is, dislocations which form during annealing[35] can serve as nucleation sites for oxidation induced stacking faults (OISF, see Chap. 2) if oxidation is carried out simultaneously with the anneal (i.e., the annealing is performed in an oxygen ambient).

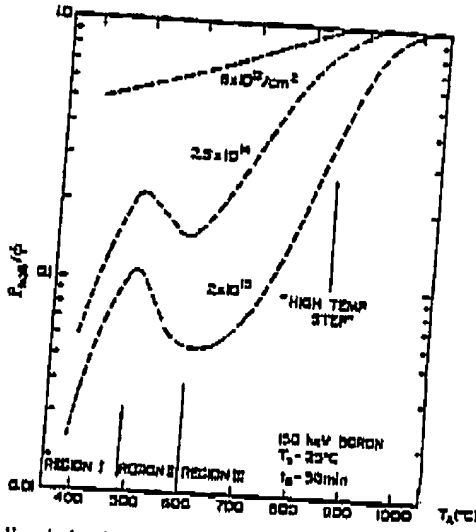

Fig. 10-20 Isochronal annealing behavior of boron. The ratio of free-carrier content, P_{Hall}, to dose ϕ is plotted against anneal temperature T_A for three doses of boron.[32] Reprinted with permission of Gordon and Breach Publishing Company.

10.3.4.3 Annealing of Amorphous Layers: The annealing of continuous amorphous layers that extend to the Si surface has been found to occur by solid-phase epitaxy (SPE),[36] at temperatures between 500–600°C (Fig. 10-21). That is, a recrystallization process occurs on the underlying crystalline substrate, and regrowth proceeds toward the surface. The amorphous layer regrows at varying rates, depending on the annealing temperature, crystal orientation, and implanted species, although at 600°C regrowth is usually completed in a matter of minutes. Regrowth is faster on (100) than (111) Si, and impurities such as B, P, and As enhance regrowth, while O, C, N, or Ar retard regrowth. In practice, 550°C is favored, since (100) regrowth at this temperature occurs at a controllable and reproducible rate.

The impurity dopant atoms are swept into substitutional lattice sites during the SPE regrowth, and thus full electrical activation within the amorphous layer can be obtained at relatively low temperatures. The impurities that are implanted into the region beyond the amorphous layer, however, must be subjected to the higher temperatures needed to electrically activate impurities in regions of primary crystalline damage (Fig. 10-22). Therefore, to fully activate an amorphous layer, and the region of heavy primary crystalline damage behind it, higher temperature anneals than 600°C must be used (normally 800–1000°C). Note that specific *minimum* times and temperatures depend on the particular implanted species and dose.

If the amorphous layer does not extend all the way to the surface (i.e., a buried amorphous layer), the annealing proceeds differently.[38] That is, SPE occurs at both amorphous-single crystal interfaces, and the regrowing interfaces meet below the surface. This meeting point has been found to be a heavily damaged layer, with properties likely to cause device degradation. Thus, it is prudent to select implantation conditions that avoid the formation of buried amorphous layers. Note that if a wafer exhibits color bands after implantation and anneal, they are probably symptomatic of a subsurface damage layer left behind by a buried amorphous

Fig. 10-21 Solid phase regrowth of a 200 keV, $6x10^{15}/cm^2$ antimony implantation at 525°C. TEM cross section micrograph. Courtesy of Institute of Physics, Conference Series.[36]

layer. The gives rise to optical interference effects from the light reflected off the subsurface damage layers and the surface.

Some of the crystalline defects in the region beyond the amorphous layer are annealed out during subsequent thermal cycles, but others give rise to extended defects (such as dislocation loops and stacking faults), which then grow and interact. Under some implantation and annealing conditions, these defects move to the surface and eventually disappear, while in others they grow into larger structures which intersect the surface or remain in the bulk.

In a large number of cases, the total number of "excess" Si atoms found in dislocation loops after thermal annealing fits a remarkably simple model. Even though hundreds to thousands of atoms are displaced from their positions in the Si lattice by each ion impact, the number of residual Si atoms left out of the lattice after the completion of thermal annealing increases with ion dose and is closely proportional to the number of ions. This is known as the "+1" model, where the number of excess Si interstitial atoms is equal to the number of implanted dopant atoms that occupy lattice sites after thermal annealing.[38,39] These Si interstitials arise from the dopant atom replacing the Si-atom in the lattice.

10.3.4.4 Dynamic Annealing Effects: The heating of the wafer during implantation can impact the implantation damage and the effects of subsequent annealing. A rise in temperature increases the mobility of the point defects caused by the damage, and this gives rise to healing of damage even as the implant process is occurring, hence the name *dynamic annealing*.[40] In the case of light ions, sufficient damage healing may occur to prevent the formation of amorphous layers, even at very high implantation doses. In the case of heavy ion implantations, dynamic annealing can cause amorphous layer regrowth during the implantation step.

A study by Prussin *et al.*,[41] showed that the wafer cooling capability of an ion implanter can impact the structure of the damage following implantation because of dynamic annealing effects. That is, if a wafer is prevented from being significantly heated above room temperature by adequate heat sinking during implantation, dynamic annealing is minimized. On the other hand, if no heat sinking is provided and wafers are allowed to rise to temperatures ~150–300°C, dynamic annealing effects can produce changes in implantation damage structures. This typically occurs in non-reproducible and unwanted ways, such as the formation of buried amorphous layers, or crystalline layers containing high densities of dislocation loops.

10.3.4.5 Diffusion of Implanted Impurities: As described in Chap. 9, the diffusion of impurities in single-crystal Si is a complex phenomenon. The diffusion of impurities in implanted Si is

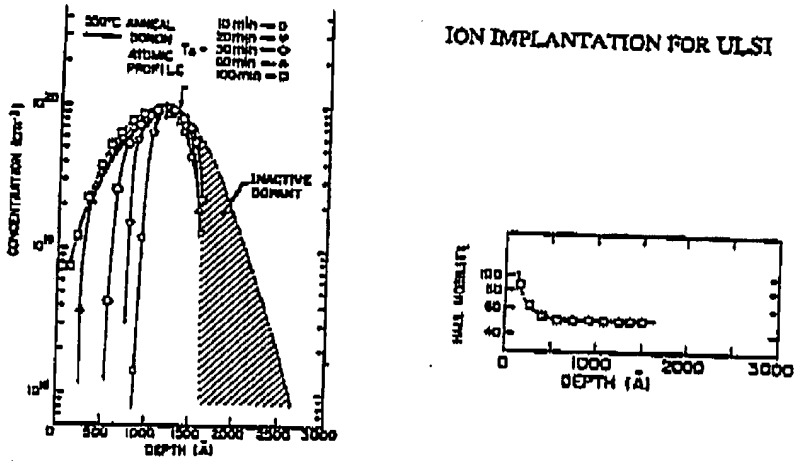

Fig. 10-22 a) Profiles for BF_2^+ implanted into <100> Si at 150 keV and $10^{15}/cm^2$ after different isothermal anneals. The dotted curve is the as-implanted atomic profile from SIMS analysis. The original amorphous-crystalline interface is denoted by the arrow. SPE is complete after ~100 minutes. The hatched region is electrically inactive.[64] b) Free-carrier concentration and mobility for implanted layers which illustrate dopant incorporation by solid phase epitaxy (SPE). Reprinted with permission of the American Physical Society.

even more complicated as a result of the presence of implantation damage. As an example, empirical studies of the *diffusion of B* in implanted single-crystal Si indicate that at high temperatures (≥ 1000°C), the data appears to obey ordinary diffusion theory (Fig. 10-23). At lower temperatures, however, ordinary diffusion theory does not accurately predict the diffusion behavior. That is, at 900°C the boron profile can be closely fit only if a diffusion constant is used that is about three times the value observed under a chemical 900°C diffusion. In addition, at 700–800°C, the depth of profile peak remains fixed, but the concentration in the tail is much deeper than is predicted from normal boron diffusion constants. This increase in the B diffusion (by as much as 4x) in the implanted profile tail occurs during the initial stage of the thermal anneal, but slows to the equilibrium diffusion rates for the rest of the anneal. Consequently, this

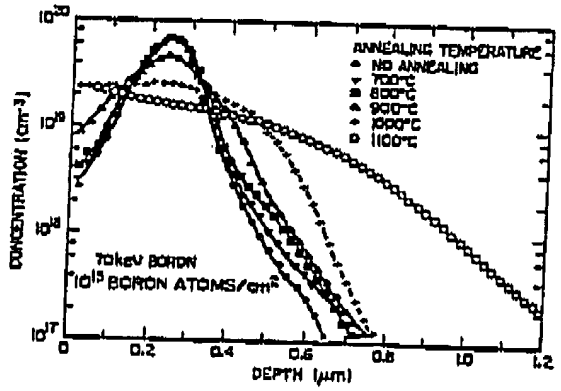

Fig. 10-23 Boron concentration as a function of annealing at various temperatures. The anneal time is 35 minutes.[5] Reprinted with permission of Philips Research Reports.

phenomenon is called *transient enhanced diffusion* (or *TED* – which is discussed in detail in Chap. 9). It is driven by the extra defects and Si interstitial atoms that are present after the implant, but which are rapidly annihilated during the first stages of thermal anneals.

In early semiconductor device fabrication processes, diffusion of impurities during annealing was often used to drive them to depths beyond the range of implantation damage. This resulted in the production of junctions which were not degraded by lattice damage. Present demands for shallow junctions in CMOS (as well as for narrow-base and shallow-emitter regions in bipolar devices), no longer allow extensive dopant redistribution during anneal. Therefore rapid thermal processing (see Chap. 8) is used to anneal implantation with minimal impurity redistribution. RTP cycles of ~1000°C for 10 sec can activate implanted layers as effectively as 30 minute furnace anneals at 1000°C (Fig. 10-24), but with impurity redistribution distances of only a few hundred angstroms (compared to several thousand angstroms for furnace anneals). RTP cycles for shallow junction annealing often use "spike" anneal temperature profiles, where a fast temperature ramp up is followed immediately by a cooling down after the anneal temperature is reached. Shallow junctions have also been fabricated by "pre-amorphizing." In which a combination implantation is performed as a way to reduce the depth of the tail from channeling. That is, an implant of Si or Ge is first carried out to amorphize the Si surface, and then the dopants (such as B) are implanted. Annealing with RTP is conducted after implanting the desired impurity (see also Sect. 11.6.4 which deals with *Shallow Junctions*).

The redistribution of impurities in polysilicon should also be considered. It is observed that dopants redistribute themselves much more rapidly in polysilicon than in single-crystal Si (as a result of grain boundary diffusion). Thus, even short RTP cycles that anneal implantations in single-crystal Si without appreciable redistribution are likely to uniformly distribute impurities throughout a thin film of polysilicon. This is useful for producing polysilicon gates with reduced boron depletion effects. For some impurities (e.g., As), a capping oxide must be present to prevent significant As outdiffusion from the polysilicon by such cycles.

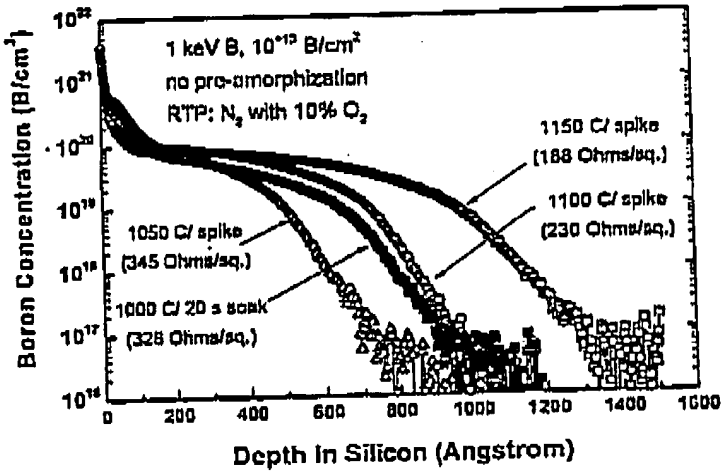

Fig. 10-24 Atomic profiles for 1 keV boron implants after a soak anneal at 1000°C for 20 sec or spike anneals at 1050°C, 1100°C, and 1150°C.[103] Reprinted with permission of Elsevier.